Ferroelectric devices created by pressure modulated stencil deposition

Paul M. te Riele, Guus Rijnders,[a] and Dave H. A. Blank
MESA+ Institute for Nanotechnology, Faculty of Science and Technology, University of Twente, P.O. Box 217, 7500 AE Enschede, The Netherlands

(Received 5 August 2008; accepted 8 October 2008; published online 10 December 2008)

Ferroelectric $Pb(Zr_xTi_{1-x})O_3$ sandwiched between $SrRuO_3$ electrodes devices were fabricated by a single stencil deposition method. By varying the pressure, the dimension of the deposited pattern could be controlled. The dimension becomes larger in the high pressure shockwave regime, which is typical for pulsed laser deposition. The particle interactions result in an increased amount of broadening. At lower pressures, the deposited material is still in the correct crystalline phase and broadening is minimized. Top electrodes are isolated from the bottom electrode by controlling the broadening of the ferroelectric medium. With this method, multilayered oxide devices can be created *in situ*. © *2008 American Institute of Physics*. [DOI: 10.1063/1.3030991]

The use of stencil techniques for structuring materials has been known for several decades[1] and has enabled direct patterning of thin films with lateral dimensions down to 40 nm, comparable with state-of-the-art e-beam lithography. So far, this technique has mainly been used for patterning of single component materials, such as metals. In case of complex oxides, conventional structuring techniques are often not suited, and direct patterning during deposition would be desirable. Typically, highly selective wet-etching chemicals are not known for multilayer oxide structures and functionality is often affected by physical dry etching techniques such as Ar-milling and focused ion beam (FIB).[2] In this paper, we used direct patterning of oxides by pulsed laser deposition (PLD) through apertures of a stencil. Structures are created by local deposition on substrates at elevated substrate temperatures. A known drawback of stencil deposition is the occurrence of broadening due to deposition in the shadowed area. The amount of broadening depends on the gap between stencil and substrate as well as the expansion mechanisms of the evaporating material, which can be controlled by pressure. The possibility to create all oxide functional devices by pressure modulated stencil deposition is presented.

Usually, stencil deposition of oxides, such as $BaTiO_3$,[3] by PLD is performed at room temperature, and an additional anneal step is required to obtain the correct crystallinity and functionality. When the depositions are done at elevated temperatures,[4] the deposition conditions are often chosen to be similar to the deposition conditions of unstructured films. Effects of broadening, which result in structures being wider than the dimensions of the apertures and eventually nonisolated structures, are often neglected. Control of the broadening is therefore essential for patterning of oxides by stencil deposition.

The used stencils consist of a silicon support with a SiN membrane. A silicon (001) wafer is coated with a low stress SiN film on both sides by low pressure chemical vapor deposition. The membrane thickness is determined by the thickness of this SiN layer and varies typically between 200 nm and 1 μm. Photoresist patterns are transferred into the SiN by reactive ion etching. A KOH wet back etch removes the Si support locally and releases the membrane. Stencil apertures can be defined by standard or deep ultra violet photolithography,[5] laser-interference lithography,[6] or directly by FIB milling.

PLD has developed into an excellent technique for the deposition of oxides.[7,8] A relatively low laser fluence (~ 2 J cm^{-2}) on stoichiometric targets results in homogeneous ablation and particulate-free films. The possibility to deposit in a high oxygen ambient pressure (~ 0.1 mbar) results in the desired kinetic energy of the arriving species and proper oxygen content in the film. Deposition on heated single crystal substrates (typical 500–800 °C) enables epitaxial thin film growth. These conditions are compatible with stencil technology since the stencils easily withstand these high temperatures and oxidizing environment.

The deposition system consists of a vacuum chamber with a base pressure of 10^{-7} mbar and a KrF excimer laser with a wavelength of 248 nm and a pulse duration of 25 ns. The beam hits the target under an angle of 45° and the substrate is mounted parallel to the target surface. For epitaxial growth studies, depositions were done on single terminated $SrTiO_3$ (001) substrates. The substrates are treated according to the procedure described in Ref. 9. This results in (001) TiO_2 terminated and atomically smooth surfaces of the substrates. As a bottom electrode, $SrRuO_3$ (SRO) is deposited at a substrate temperature of 600 °C, 58 mm target substrate separation, and 0.13 mbar of oxygen. The fluence and spot size were kept constant for all deposition at 2.5 J/cm^2 and 3.0 mm^2. The resulting bottom electrode is a 75 nm thick, fully coherent, atomically smooth film.

Best crystallinity and functionality of $Pb(Zr_{0.48}Ti_{0.52})O_3$ (PZT) are obtained for films deposited at 600 °C and 0.13 mbar of oxygen. However, when the PZT is patterned by stencil deposition under these conditions, extreme broadening is observed and functionality is lost. This is shown in Fig. 1(a) where isolated structures cannot be distinguished when the material is deposited through a stencil with 1×3 μm^2 rectangular apertures. The gap between stencil and substrate is checked optically and found to be similar for all experiments on the order of 1–3 μm. As mentioned above, the broadening in PLD stencil deposition is highly pressure dependent as can be seen in Figs. 1(b) and 1(c). Isolated structures can be obtained below 0.1 mbar and there is an abrupt transition between 0.1 and 0.13 mbar. By lowering the

[a]Electronic mail: a.j.h.m.rijnders@utwente.nl.

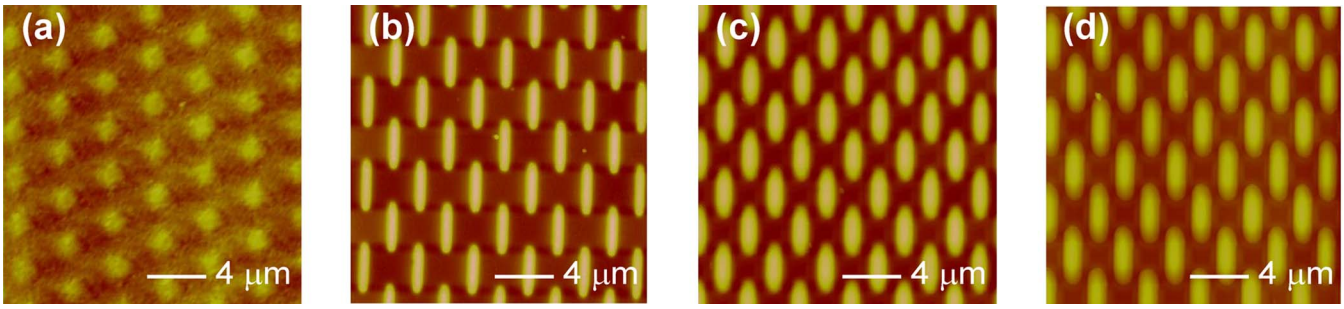

FIG. 1. (Color online) PZT deposited through a stencil with rectangular apertures (1×3 μm^2) at 400 °C and (a) 0.13, (b) 0.10, (c) 0.05, and (d) 0.013 mbar of oxygen. In all experiments the same amount of material is deposited at 2 Hz for 45 min.

pressure, not only the broadening is minimized, but also the functionality is restored. In case of stencil deposition, the best crystallinity of the material is obtained at lower temperatures (400–500 °C) as was checked by x-ray diffraction. In the low pressure regime, material is mainly broadened by geometrical effects and surface diffusion. Geometrical broadening can be described by $\delta=2(R+r)G/D$ (Ref. 10) in which R is the dimension of the spot of evaporation, r is the dimension of the aperture in the stencil, G is the gap, D is the target-substrate separation, and δ is the resulting structure broadening. This effect is proportional to the gap between stencil and substrate and inversely proportional to the target substrate separation. The relation between the gap and the amount of broadening has been examined for PLD but does not show this proportionality. This is explained by the highly forwarded particle flux in PLD. Generally geometrical broadening models[10] are based on homogeneous evaporation with a $\cos^n(\theta)$, $n=0-2$ distribution. This, however, is not the case for PLD in a low pressure environment where typically a $\cos^n(\theta)$ flux distribution with $n\sim5-15$ is found.[11,12] Therefore, the effect of the exact gap is of hardly any influence on the amount of broadening present.

In order to quantify the amount of broadening, depositions have been done through stencils with various aperture dimensions. Since the total volume propagating through the stencil per unit area is constant, the total height of the structure is depending on the width of the structure. Relatively more material is needed in the broadened edge for smaller apertures. This is shown in Fig. 2 where the [Fig. 2(a)] cross sections of the structures deposited at 0.05 mbar are given and [Fig. 2(b)] the structure width versus height is plotted for all pressures. Below a certain critical width the height of the structure is affected by the amount of broadening. For the low pressures (0.01, 0.05, and 0.1 mbar) this critical width is

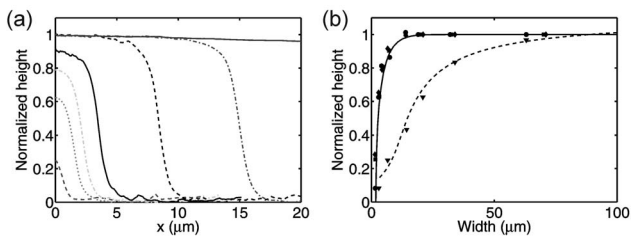

FIG. 2. (a) The cross-sectional data from the AFM analyses showing the decrease in height for the smaller structures for deposition done at 0.05 mbar. (b) The structure width as a function of height for (●) 0.01 mbar, (◆) 0.05 mbar, (■) 0.1 mbar, and (▼) 0.13 mbar of deposition pressure. For 0.01, 0.05, and 0.1 mbar a fit is made with the convolution model; for the 0.13 mbar a fit is made with shockwave.

10 μm while it is ~100 μm at 0.13 mbar. The height is normalized to exclude effects of reduced deposition rate at higher pressures. Structures below the critical width can be obtained, but the deposition rate is reduced due to the broadening effects. Pattern dimension down to 200 nm can be obtained when the deposition parameters are optimized to minimize the broadening effects.

The amount of broadening in the low pressure regime can be modeled by a convolution between the high order $\cos^n(\theta)$ angular flux distribution and the width of the aperture. The data are fitted to this convolution model and are included in Fig. 2 by the black line. This model cannot be used to fit the data in the 0.13 mbar case since the amount of broadening is depending on the size of the aperture. For the 0.13 mbar experiment, a shockwave is formed[12,13] and the particle interaction in the leading edge of the plume results in lower n values of the expanding plasma. Whereas at low pressures, the origin of the angular distribution is located close to the target surface; at high pressures it is located in the stencil apertures. In the latter case, the material flux expands homogeneously from the aperture entrance. By integration over all the point sources inside the aperture, a model is created for this high pressure regime, depicted in Fig. 2 by the dashed line.

This clear dependence of broadening on process pressure can be used to create multilayered structures in a single processing step. This is demonstrated by the fabrication of an all-oxide ferroelectric (FE) capacitor, consisting of PZT sandwiched between SRO electrodes. To prevent electrical shorts between the top and bottom electrode, we have introduced a broadened insulating PZT layer. After the deposition of the FE PZT at 0.075 mbar (45 min at 2 Hz), the insulating layer is deposited at 0.13 mbar (5 min at 2 Hz). Afterward the SRO is deposited at 0.025 mbar to create the top electrode. The depositions were performed at a substrate temperature of 500 °C, which was optimized in these experiments for the FE remnant polarization. A schematic cross section of the resulting 100×100 μm^2 device is shown in Fig. 3(a). Figure 3(b) shows the total induced polarization versus the applied voltage. The device shows symmetrical FE switching behavior, although some leakage through the device is measured at high fields. A remnant polarization of 6 $\mu C/cm^2$ is observed if the total induced polarization is corrected for the leakage through the device.

In summary, stencil deposition can be combined with PLD for creating all-oxide devices. However, at typical deposition conditions, extreme broadening of the patterns can be observed. These broadening effects are highly pressure dependent and the formation of a shockwave should be

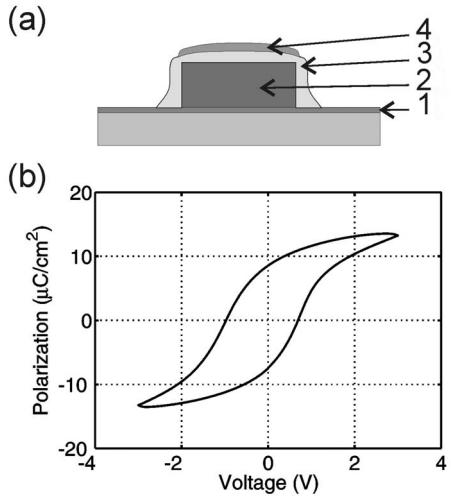

FIG. 3. (a) FE device based on PZT deposited in a single step through a stencil. The FE PZT (2) is deposited at 0.075 mbar of oxygen and the PZT the 0.13 mbar acts as an insulating barrier (3). The top electrode (4) is deposited at 0.025 mbar. (b) Polarization as a function of applied voltage over the device.

prevented. However, the broadening effects can be utilized to create multilayered devices in a single step. Here, we have used this method to create all-oxide FE devices.

The partial support of the EC-funded project NaPa (Contract No. NMP4-CT-2003-500120) is gratefully acknowledged. The content of this work is the sole responsibility of the authors.

[1]G. J. Dolan, Appl. Phys. Lett. **31**, 337 (1977).
[2]C. S. Ganpule, A. Stanishevsky, Q. Su, S. Aggarwal, J. Melngailis, and E. Williams, Appl. Phys. Lett. **75**, 409 (1999).
[3]C. V. Cojocaru, C. Harnagea, F. Rosei, A. Pignolet, M. A. F. van den Boogaart, and J. Brugger, Appl. Phys. Lett. **86**, 183107 (2005).
[4]H. J. Shin, J. H. Choi, H. J. Yang, Y. D. Park, Y. Kuk, and C. J. Kang, Appl. Phys. Lett. **87**, 113114 (2005).
[5]M. A. F. van den Boogaart, G. M. Kim, R. Pellens, J. P. van den Heuvel, and J. Brugger, J. Vac. Sci. Technol. **22**, 3174 (2004).
[6]C. J. M. van Rijn, G. J. Veldhuis, and S. Kuiper, Nanotechnology **9**, 343 (1998).
[7]D. Dijkkamp, T. Venkatesan, X. D. Wu, S. A. Shaheen, N. Jisrawi, Y. H. Min-Lee, L. McLean, and M. Croft, Appl. Phys. Lett. **51**, 619 (1987).
[8]G. Rijnders, D. H. A. Blank, J. Choi, and C.-B. Eom, Appl. Phys. Lett. **84**, 505 (2004).
[9]G. Koster, B. L. Kropman, G. J. H. M. Rijnders, D. H. A. Blank, and H. Rogalla, Appl. Phys. Lett. **73**, 2920 (1998).
[10]N. Takano, L. M. Doeswijk, M. A. F. van den Boogaart, J. Auerswald, H. F. Knapp, O. Dubochet, T. Hessler, and J. Brugger, J. Micromech. Microeng. **16**, 1606 (2006).
[11]B. Toftmann, J. Schou, and J. G. Lunney, Phys. Rev. B **67**, 104101 (2003).
[12]C. J. Druffner and G. P. Perram, *MRS Symposia Proceedings No. EXS-3*, EE5.2.1 (Materials Research Society, Pittsburgh, 2004).
[13]D. B. Geohegan, Thin Solid Films **220**, 138 (1992).